

Probing $|V_{cs}|$ and lepton flavor universality through $D \rightarrow K_0^*(1430)\ell\nu_\ell$ decay

Yin-Long Yang*, Hai-Jiang Tian*, Ya-Xiong Wang, Hai-Bing Fu,[†] Tao Zhong,[‡] and Sheng-Quan Wang[§]
Department of Physics, Guizhou Minzu University, Guiyang 550025, P.R.China

Dong Huang

Center of Experimental Training, Guiyang Institute of Information Science and Technology, Guiyang 550025, P.R.China

In this paper, we calculate the semileptonic decay $D \rightarrow K_0^*(1430)\ell\nu_\ell$ with $\ell = (e, \mu)$ induced by $c \rightarrow s\ell\nu_\ell$ transition. For the key component, $D \rightarrow K_0^*(1430)$ transition form factors (TFFs) $f_\pm(q^2)$ are calculated within the framework of QCD light-cone sum rule. Then, we consider two scenarios for $K_0^*(1430)$ -meson twist-2 distribution amplitude. For the scenario 1 (S1), we take the truncated form based on Gegenbauer polynomial series. Meanwhile, we also consider the scenario 2 (S2) constructed by light-cone harmonic oscillator model, where the model parameters are fixed by the $K_0^*(1430)$ -meson twist-2 distribution amplitude 10th-order ξ -moments calculated by using the background field theory. For the TFFs at large recoil point, we have $f_+^{(S1)}(0) = 0.597_{-0.121}^{+0.122}$ and $f_-^{(S1)}(0) = -0.136_{-0.035}^{+0.023}$, $f_+^{(S2)}(0) = 0.663_{-0.134}^{+0.135}$ and $f_-^{(S2)}(0) = -0.202_{-0.046}^{+0.026}$. After extrapolating TFFs to the whole physical q^2 -region, we calculate the branching fractions of $D^0 \rightarrow K_0^{*+}(1430)\ell^-\bar{\nu}_\ell$ and $D^+ \rightarrow K_0^{*0}(1430)\ell^+\nu_\ell$ which at 10^{-4} -order level for the S1 and S2 cases. Meanwhile, we predict the CKM matrix $|V_{cs}|^{(S1)} = 0.997_{-0.172}^{+0.258}$, $|V_{cs}|^{(S2)} = 0.903_{-0.155}^{+0.233}$, and lepton flavor universality $\mathcal{R}_{K_0^*}^{(S1)} = 0.768_{-0.368}^{+0.560}$, $\mathcal{R}_{K_0^*}^{(S2)} = 0.764_{-0.365}^{+0.555}$. Finally, we discuss the angular observables of forward-backward asymmetries, lepton polarization asymmetries and q^2 -differential flat terms for this decay.

PACS numbers:

I. INTRODUCTION

As the lightest particle containing the c -quark, the exclusive semileptonic decay processes of D meson are highly valuable in enhancing our understanding of weak and strong interactions within the framework of the Standard Model (SM). The Cabibbo-Kobayashi-Maskawa (CKM) matrix elements describe the flavor-changing transitions involving quarks, that can be determined by semileptonic decays. The binding effect of strong interaction is limited to hadronic current, which can be parameterized by the form factors, which are viewed as one of the most important precision tests of the SM [1]. From this point, the semileptonic decay of charm mesons plays an important role in the determination of CKM matrix elements Cabibbo-favored $|V_{cs}|$ and Cabibbo-suppressed $|V_{cd}|$.

Experimentally, the charmed D -meson semileptonic decay processes have been measured by the BESIII collaboration [2–9] and CLEO Collaboration [10–14], etc. In which, for $D \rightarrow P, V + \ell\nu_\ell$ (P and V stand for pseudoscalar and vector mesons respectively), its discussion is quite mature now and the experimental and theoretical groups are still trying to improve the accuracy of the relevant calculations. The precision of the

measurement has been continuously improved in recent years. However, there are few experimental studies on scalar mesons. It is known that only BESIII [15–20] and CLEO [12, 21] have studied the semileptonic decays of $D_{(s)}$ to $a_0(980)$, $f_0(500)$ or $f_0(980)$, which all involve only u and d quark, without considering scalar mesons containing s quark. Particularly for D -meson semileptonic decay into one scalar meson, BESIII collaboration reported the $D^{0(+)} \rightarrow a_0(980)^{-(0)}e^+\nu_e$ decay with significance of 6.4σ and 2.9σ respectively by utilizing the e^+e^- collision data sample of 2.93 fb^{-1} collected at a center-of-mass energy of 3.773 GeV with the order of the absolute branching fractions are 10^{-4} [16]. Recently, the BESIII collaboration measured a branching ratio of 10^{-3} for $D_s^+ \rightarrow f_0(980)e^+\nu_e$ based on a data with integrated luminosity of 7.33 fb^{-1} at 4.128 and 4.226 GeV [17]. Presently, for scalar mesons like $a_0(980)$ and $f_0(980)$, despite the remarkable progress made by the quark model in explaining the majority of hadronic states over the past decades, their internal structures have remained a subject of intense theoretical and experimental scrutiny and controversy. As for semileptonic decay $D \rightarrow K_0^*(1430)\ell\nu_\ell$, FOCUS collaboration presented the ratio $\Gamma(D^+ \rightarrow \bar{K}_0^*(1430)^0\mu^+\nu)/\Gamma(D^+ \rightarrow K^-\pi^+\mu^+\nu) < 0.64\%$, which is from the discussion about the Hadronic Mass Spectrum Analysis of $D^+ \rightarrow K^-\pi^+\mu^+\nu$ [22]. Till now, there is no experimental result for $D \rightarrow K_0^*(1430)\ell\nu_\ell$ directly.

Currently, the internal structure of scalar mesons is considered to be in the form of $q\bar{q}$ states [23], $qq\bar{q}\bar{q}$ states [24], molecular states [25], glueball states [26] or hybrid states [27]. In order to facilitate the study of scalar mesons, two viable and publicly acceptable theo-

*Yin-Long Yang and Hai-Jiang Tian contributed equally to this work.

[†]Electronic address: fuhb@gzmu.edu.cn (corresponding author)

[‡]Electronic address: zhongtao1219@sina.com

[§]Electronic address: sqwang@cqu.edu.cn

retical schemes have been proposed as methods for investigating them [28–31]. For one picture, the light scalar mesons $f_0(980)$, $a_0(980)$, κ , etc., are seen as the ground $q\bar{q}$ states, and nonet mesons near 1.5 GeV are interpreted as the first excited states. For another picture, $f_0(1370)$, $a_0(1450)$, $K_0^*(1430)$, etc., are treated as lowest-lying P -wave $q\bar{q}$ states and nonet mesons below 1 GeV are viewed as four-quark bound states [32–36]. For the scalar mesons, $K_0^*(1430)$ -meson in the charmed meson semileptonic decays still have no experimental results in comparing with $a_0(980)$ and $f_0(980)$. Meanwhile, the $K_0^*(1430)$ -meson is considered as the diquark state from most theoretical researches [37–45], and the observables for the decay processes with $K_0^*(1430)$ final state can provide valuable insights for further understanding the internal nature of scalar meson. So, it is meaningful to have a deep look into the semileptonic $D \rightarrow K_0^*(1430)\ell\nu_\ell$ with $c \rightarrow s\ell\nu_\ell$ transition, where the $K_0^*(1430)$ -meson is treated as a $s\bar{q}$ or $q\bar{s}$ state for computational discussion.

Furthermore, the $D \rightarrow K_0^*(1430)$ transition form factors (TFFs) are crucial components in this decay within the SM, which can be calculated by various non-perturbative method, such as three-point QCD sum rule [45], covariant light-front approach (CLF) [46] and generalized factorization model (GFM) [47]. Normally, the light-cone sum rule (LCSR) approach is suitable for calculating the heavy-to-light TFFs, with which the non-local operators matrix element are parameterized into the light-cone distribution amplitudes with increasing twist. In our previous work, the $D_s \rightarrow K_0^*(1430)$ with $c \rightarrow d$ transition have been studied by the LCSR approach [48]. So the Cabibbo-favored channel $D \rightarrow K_0^*(1430)$ with $c \rightarrow s$ transition can also be researched by the LCSR approach, which is the motivation in this paper.

As one of the most important non-perturbative parameters, $K_0^*(1430)$ -meson LCDAs including long-distance dynamics at lower energy scale are critical to the behavior of TFFs. Thus, a detailed investigation of LCDAs is conducive to enhancing the precision of the calculation of TFFs. Theoretically, the QCDSR [23] and CLF approach [49] present the $K_0^*(1430)$ -meson leading-twist LCDAs. As we know, the $K_0^*(1430)$ -meson leading-twist LCDA can be expanded with a series of Gegenbauer coefficients (also called Gegenbauer moments), which can be calculated by the QCD sum rule approach. One often take the first few order Gegenbauer moments which lead to the truncated form (TF) to avoid false oscillation from the higher order moments. Such as the pion and kaon twist-2 LCDA up to second order calculated by QCDSR [50], ρ , K^* , ϕ -meson longitudinal and transverse leading-twist LCDAs up to second order from QCDSR [51]. Recently, the Lattice QCD proved the effectiveness of the TF from [50, 52]. Meanwhile, we have calculated the first ten-order ξ -moments of $K_0^*(1430)$ -meson leading-twist LCDA by using the QCDSRs within the framework of background field theory [48]. Thus, in this paper, we will take the first three order Gegenbauer moments to make the TF, which is called scenario

1 (S1). On the other hand, one will take the nature light-cone harmonic oscillator (LCHO) model to describe the behavior of $K_0^*(1430)$ -meson leading-twist LCDA, which is considered as scenario 2 (S2) of our study. The model-dependent parameters can be fixed by the first ten-order ξ -moments at scale $\mu_k = 1.4$ GeV. By comparing the observables of semileptonic decay $D \rightarrow K_0^*(1430)\ell\nu_\ell$ under the two different forms of $K_0^*(1430)$ meson leading-twist LCDA, it is helpful to see which one have a better behavior in this semileptonic decays. This will not only test the SM but also test the accuracy of our determination of DA parameters. Particularly, in order to make the behavior of TFFs for $D \rightarrow K_0^*(1430)$ more precise, we need to consider the contribution of twist-3 DAs $\phi_{3;K_0^*}^{p,\sigma}(x, \mu)$. The twist-3 DAs based on Gegenbauer series expansion are also calculated within the framework of the background field theory in our early previous work [53], which will be reuse here.

II. THEORETICAL FRAMEWORK

To express the full spectrum of $D \rightarrow K_0^*(1430)\ell\nu_\ell$ decays, one can start with the simple form for differential decay width with respect to the squared momentum transfer q^2 and the angle $\cos\theta_\ell$ between the direction of flight of $K_0^*(1430)$ and ℓ in the center of mass frame of $\ell\nu_\ell$, which have the following form

$$\frac{d^2\Gamma}{dq^2 d\cos\theta_\ell} = \frac{1}{32(2\pi)^3 m_D^2} |\mathbf{q}| \left(1 - \frac{m_\ell^2}{q^2}\right) \times |\mathcal{M}(D \rightarrow K_0^*(1430)\ell\nu_\ell)|^2. \quad (1)$$

In which, the symbol \mathbf{q} stands for the three-momentum of the $\ell\nu_\ell$ pair in the D -meson rest frame. To write the amplitude $\mathcal{M}(D \rightarrow K_0^*(1430)\ell\nu_\ell)$ explicitly, we decompose the non-vanishing hadronic matrix elements of the quark operators in the effective Hamiltonian *i.e.* $\mathcal{H}_{\text{eff}} = \frac{G_F}{\sqrt{2}} V_{cs} \bar{c}\gamma_\mu(1 - \gamma_5)s\bar{\ell}\gamma^\mu(1 - \gamma_5)\nu_\ell$ in terms of the Lorentz invariant hadronic form factors $f_+(q^2)$ and $f_0(q^2)$ with the definition

$$\begin{aligned} \langle K_0^*(p) | \bar{s}\gamma_\mu\gamma_5 c | D(p+q) \rangle &= \left[(2p+q)_\mu - \frac{m_D^2 - m_{K_0^*}^2}{q^2} q_\mu \right] \\ &\times f_+(q^2) + \frac{m_D^2 - m_{K_0^*}^2}{q^2} q_\mu f_0(q^2). \end{aligned} \quad (2)$$

The full differential decay rate for the $D \rightarrow K_0^*(1430)\ell\nu_\ell$ semileptonic decay can be expressed as $d^2\Gamma/(dq^2 d\cos\theta_\ell) = a_{\theta_\ell}(q^2) + b_{\theta_\ell}(q^2)\cos\theta_\ell + c_{\theta_\ell}(q^2)\cos^2\theta_\ell$, with the angular coefficient functions are [54]

$$\begin{aligned} a_{\theta_\ell}(q^2) &= \mathcal{N}_{\text{ew}} \lambda^{3/2} \left(1 - \frac{m_\ell^2}{q^2}\right)^2 \left[|f_+(q^2)|^2 + \frac{1}{\lambda} \frac{m_\ell^2}{q^2} \right. \\ &\times \left. \left(1 - \frac{m_{K_0^*}^2}{m_D^2}\right)^2 |f_0(q^2)|^2 \right], \end{aligned}$$

$$\begin{aligned}
b_{\theta_\ell}(q^2) &= 2\mathcal{N}_{\text{ew}}\lambda \left(1 - \frac{m_\ell^2}{q^2}\right)^2 \frac{m_\ell^2}{q^2} \left(1 - \frac{m_{K_0^*}^2}{m_D^2}\right) \\
&\quad \times \text{Re}[f_+(q^2)f_0^*(q^2)], \\
c_{\theta_\ell}(q^2) &= -\mathcal{N}_{\text{ew}}\lambda^{3/2} \left(1 - \frac{m_\ell^2}{q^2}\right)^3 |f_+(q^2)|^2. \quad (3)
\end{aligned}$$

In which, G_F is the Fermi constant, m_ℓ and θ_ℓ are lepton mass and helicity angle, $\mathcal{N}_{\text{ew}} = G_F^2 |V_{cs}|^2 m_D^3 / 256\pi^3$ and $\lambda \equiv \lambda(1, m_{K_0^*}^2/m_D^2, q^2/m_D^2)$ with $\lambda(a, b, c) \equiv a^2 + b^2 + c^2 - 2(ab + ac + bc)$. With $f_0(q^2) = f_+(q^2) + q^2/(m_D^2 - m_{K_0^*}^2)f_-(q^2)$, $f_\pm(q^2)$ are the $D \rightarrow K_0^*(1430)$ TFFs. After integrating over the helicity angle $\theta_\ell \in [-1, 1]$, the differential decay width of $D \rightarrow K_0^*(1430)\ell\nu_\ell$ over q^2 with respect to kinematic variables q^2 can be written as,

$$\begin{aligned}
\frac{d\Gamma}{dq^2} &= \frac{G_F^2 |V_{cs}|^2 m_D^3}{192\pi^3} \lambda^{3/2} \left(1 - \frac{m_\ell^2}{q^2}\right)^2 \left\{ \left(1 + \frac{m_\ell^2}{2q^2}\right) \right. \\
&\quad \times |f_+(q^2)|^2 + \frac{1}{\lambda} \frac{3m_\ell^2}{2q^2} \left(1 - \frac{m_{K_0^*}^2}{m_D^2}\right)^2 |f_0(q^2)|^2 \left. \right\}. \quad (4)
\end{aligned}$$

Furthermore, one can calculate three independent observables from three angular coefficient functions $a_{\theta_\ell}(q^2), b_{\theta_\ell}(q^2), c_{\theta_\ell}(q^2)$, *i.e.*, forward-backward asymmetries, lepton polarization asymmetries and flat terms. These observables are very sensitive to beyond the Standard Model (BSM) physics. So, one can extract results of three observables from $D \rightarrow K_0^*\ell\nu_\ell$ through the relationship between these observables and TFF, *i.e.*, [55]

$$\begin{aligned}
\mathcal{A}_{\text{FB}}(q^2) &= \left[\frac{1}{2}b_{\theta_\ell}(q^2)\right] : \left[a_{\theta_\ell}(q^2) + \frac{1}{3}c_{\theta_\ell}(q^2)\right], \\
\mathcal{A}_{\lambda_\ell}(q^2) &= 1 - \frac{2}{3} \left\{ \left[3\left(a_{\theta_\ell}(q^2) + c_{\theta_\ell}(q^2)\right) \right. \right. \\
&\quad \left. \left. + \frac{2m_\ell^2}{q^2 - m_\ell^2}c_{\theta_\ell}(q^2)\right] : \left[a_{\theta_\ell}(q^2) + \frac{1}{3}c_{\theta_\ell}(q^2)\right] \right\}, \\
\mathcal{F}_{\text{H}}(q^2) &= \left[a_{\theta_\ell}(q^2) + c_{\theta_\ell}(q^2)\right] : \left[a_{\theta_\ell}(q^2) + \frac{1}{3}c_{\theta_\ell}(q^2)\right]. \quad (5)
\end{aligned}$$

The above observables are functions of the ratio of TFFs. So next step, we calculate the TFFs by using LCSR and start with the the following correlator

$$\Pi_\mu(p, q) = i \int d^4x e^{iq \cdot x} \langle K_0^*(p) | T \{ j_{2\mu}(x), j_1(0) \} | 0 \rangle \quad (6)$$

where $j_{2\mu}(x) = \bar{q}_2(x)\gamma_\mu\gamma_5 c(x)$ and $j_1(0) = \bar{c}(0)i\gamma_5 q_1(0)$. $q_{1,2}$ present the light quark, $q_2 = s$, $q_1 = d$ is for $D^+ \rightarrow K_0^{*0}$ and $q_1 = u$ is for $D^0 \rightarrow K_0^{*+}$, where $m_d \sim m_u \sim 0$, the results of TFFs are almost the same. In the time-like q^2 -region, we can insert a complete intermediate state with D -meson quantum numbers into the correlator (6) and separate the pole term of the lowest D -meson to obtain the hadronic representation. By using the hadronic dispersion relations, the $D \rightarrow K_0^*$ matrix element also can be derived. In the space-like q^2 -region, we carry out the operator product expansion (OPE) near the light-cone $x^2 \rightsquigarrow 0$, where the light-cone expansion of the

c -quark propagator retains only the two-particle, while twists higher than three are neglected, as the contributions from the remaining components are small and can reasonably be neglected. After separating all the continuum states and excited states by introducing a effective threshold parameter s_D and using the Borel transformation, the TFF can be obtained, which has a similar expression to Ref. [48], in which, we repeat the corresponding calculation process and get the same results. For the brevity of this short essay, we will not provide specific expressions here.

Then, $K_0^*(1430)$ -meson twist-2 and twist-3 LCDAs are the main nonperturbative uncertainty for TFFs. For scalar meson DAs, under the premise of following to the principle of conformal symmetry hidden in the QCD Lagrangian, they can be systematically expanded into a series of Gegenbauer polynomials with increasing conformal spin [56]. The first twist-2 DA $\phi_{2;K_0^*}^{(S1)}(x, \mu)$ based on TF model can be expressed in the following formulations

$$\phi_{2;K_0^*}^{(S1)}(x, \mu) = 6x\bar{x} \sum_{n=0}^{N=3} a_n^{2;K_0^*}(\mu) C_n^{3/2}(\xi). \quad (7)$$

Here, $C_n^{3/2}(\xi)$ is the Gegenbauer polynomial with $\xi = 2x - 1$ and the zeroth order Gegenbauer moment $a_0^{2;K_0^*}(\mu)$ is equal to 0 for scalar mesons and the behavior of the DA is mainly determined by the odd Gegenbauer moment.

In addition, we constructed the twist-2 DA by using LCHO model. The wave function (WF) of the $K_0^*(1430)$ are obtained based on the Brodsky-Huang-Lepage (BHL) description which postulate that a correlation exists between the equal-time WF in the rest frame and the light-cone WF. The leading-twist WF can be expressed as $\Psi_{2;K_0^*}(x, \mathbf{k}_\perp) = \chi_{2;K_0^*}(x, \mathbf{k}_\perp) \Psi_{2;K_0^*}^R(x, \mathbf{k}_\perp)$. After determining the scalar meson $K_0^*(1430)$ total spin-space WF $\chi_{2;K_0^*}(x, \mathbf{k}_\perp)$ and spatial WF $\Psi_{2;K_0^*}^R(x, \mathbf{k}_\perp)$ [57], we have following expression by using the relation between $K_0^*(1430)$ leading-twist DA and WF, $\phi_{2;K_0^*}(x, \mu) = \int_{|\mathbf{k}_\perp|^2 \leq \mu^2} \frac{d^2\mathbf{k}_\perp}{16\pi^3} \Psi_{2;K_0^*}(x, \mathbf{k}_\perp)$, to integrate over the transverse momentum \mathbf{k}_\perp , and get the following expression

$$\begin{aligned}
\phi_{2;K_0^*}^{(S2)}(x, \mu) &= \frac{A_{2;K_0^*} \beta_{2;K_0^*} \tilde{m}}{4\sqrt{2}\pi^{3/2}} \sqrt{x\bar{x}} \varphi_{2;K_0^*}(x) \\
&\quad \times \exp \left[-\frac{\hat{m}_q^2 x + \hat{m}_s^2 \bar{x} - \tilde{m}^2}{8\beta_{2;K_0^*}^2 x\bar{x}} \right] \\
&\quad \times \left\{ \text{Erf} \left(\sqrt{\frac{\tilde{m}^2 + \mu^2}{8\beta_{2;K_0^*}^2 x\bar{x}}} \right) - \text{Erf} \left(\sqrt{\frac{\tilde{m}^2}{8\beta_{2;K_0^*}^2 x\bar{x}}} \right) \right\}. \quad (8)
\end{aligned}$$

In which, $\tilde{m} = \hat{m}_q x + \hat{m}_s \bar{x}$ with $\hat{m}_s = 370$ MeV and $\hat{m}_q = 250$ MeV are constituent quark, $\bar{x} = (1 - x)$ and $\hat{B}_{2;K_0^*} \simeq -0.025$ is determined by $\langle \xi_{2;K_0^*}^2 \rangle / \langle \xi_{2;K_0^*}^1 \rangle$ whose rationality can be judged by the goodness of fit. Obviously, the behavior of $\phi_{2;K_0^*}^{(S2)}(x, \mu)$ is determined by

unknown model parameters $A_{2;K_0^*}$, $\alpha_{2;K_0^*}$ and $\beta_{2;K_0^*}$ and function $\varphi_{2;K_0^*}(x) = (x\bar{x})^{\alpha_{2;K_0^*}} \left[C_1^{3/2}(\xi) + \hat{B}_{2;K_0^*} C_2^{3/2}(\xi) \right]$. $\varphi_{2;K_0^*}(x)$ determines the WF's longitudinal distribution by factor $(x\bar{x})^{\alpha_{2;K_0^*}}$ which is close to asymptotic form $\phi_{2;K_0^*}^{(S1)}(x, \mu \rightarrow \infty) = 6x\bar{x}$. Its rationality have been discussed in Ref. [58]. The unknown model parameters $A_{2;K_0^*}$, $\alpha_{2;K_0^*}$ and $\beta_{2;K_0^*}$ can be obtained by fitting the first ten ξ -moment of $K_0^*(1430)$ through the least squares method and using the definition $\langle \xi_{2;K_0^*}^n \rangle|_\mu = \int_0^1 dx \xi^n \phi_{2;K_0^*}(x, \mu)$. For specific fitting process can be found in Refs. [57, 58]. Corresponding $\langle \xi_{2;K_0^*}^n \rangle|_\mu$ have been calculated based BFT which describes the nonperturbative effects through the vacuum expectation values of the background fields and the calculable perturbative effects by quantum fluctuations, the calculation also can be simplify through various gauge conditions. Compared to the traditional SVZ sum rules, the reliability of result $a_n^{2;K_0^*}(\mu)$ can be improved to a certain extent on this basis.

Finally, the twist-3 DAs $\phi_{3;K_0^*}^p(x, \mu)$ and $\phi_{3;K_0^*}^\sigma(x, \mu)$ for scalar mesons also can be expanded into a series of Gegenbauer polynomials [39, 59],

$$\phi_{3;K_0^*}^p(x, \mu) = 1 + \sum_{n=1}^{\mathcal{N}=2} a_{n,p}^{3;K_0^*}(\mu) C_n^{1/2}(\xi), \quad (9)$$

$$\phi_{3;K_0^*}^\sigma(x, \mu) = 6x\bar{x} \left[1 + \sum_{n=1}^{\mathcal{N}=2} a_{n,\sigma}^{3;K_0^*}(\mu) C_n^{3/2}(\xi) \right]. \quad (10)$$

where $a_{n,p/\sigma}^{3;K_0^*}(\mu)$ are determined by the relationship with $\langle \xi_{3;K_0^*}^{p(\sigma);n} \rangle$ which are also calculated by BFT method.

III. NUMERICAL ANALYSIS

In order to carry out the next calculation, we adopt following basic input parameters: the quark masses $m_c(\bar{m}_c) = 1.27 \pm 0.02$ GeV, $m_d = 4.67_{-0.17}^{+0.48}$ MeV and $m_u = 2.16 \pm 0.07$ MeV at $\mu = 2$ GeV, the meson masses $m_{D^0} = 1864.84 \pm 0.05$ MeV, $m_{D^+} = 1869.66 \pm 0.05$ MeV and $m_{K_0^*} = 1425 \pm 50$ MeV, the decay constants $f_{K_0^*} = 427 \pm 85$ MeV at $\mu_0 = 1$ GeV and $f_D = 208.4 \pm 1.5$ MeV [60].

Next step, for this part of the undetermined parameters of two twist-2 DAs, we calculated the moments $\langle \xi_{2;K_0^*}^n \rangle|_\mu$ with $n = (1, 2, 3, \dots, 10)$ in the framework of BFT, and nonperturbative vacuum condensates are up to dimension-six. Then, the Gegenbauer moments $a_n^{2;K_0^*}(\mu)$ of twist-2 DA $\phi_{2;K_0^*}^{(S1)}(x, \mu)$ based on truncated form can be determined by the relationship between with $\langle \xi_{2;K_0^*}^n \rangle|_\mu$. Therefore, we have following results at $\mu_k = \sqrt{m_D^2 - m_c^2} \approx 1.4$ GeV [48]

$$a_1^{2;K_0^*}(\mu_k) = -0.408_{-0.111}^{+0.087}, \quad a_2^{2;K_0^*}(\mu_k) = -0.018_{-0.016}^{+0.013},$$

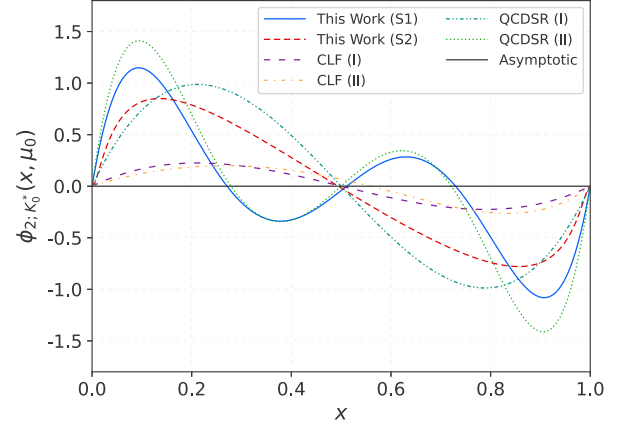


FIG. 1: Two scenarios for the $K_0^*(1430)$ -meson twist-2 DA at initial scale $\mu_0 = 1$ GeV. As a comparison, the QCDSRs [23] and CLF [49] are also presented.

$$a_3^{2;K_0^*}(\mu_k) = -0.321_{-0.072}^{+0.048}. \quad (11)$$

In addition, the optimal model parameters $A_{2;K_0^*}$, $\alpha_{2;K_0^*}$ and $\beta_{2;K_0^*}$ of $\phi_{2;K_0^*}^{(S2)}(x, \mu)$ constructed by LCHO model are obtained by fitting the first tenth order $\langle \xi_{2;K_0^*}^n \rangle|_{\mu_k}$ -moments with the least squares method at $\mu_k = 1.4$ GeV [48]

$$\begin{aligned} A_{2;K_0^*} &= -147 \text{ GeV}^{-1}, & \alpha_{2;K_0^*} &= 0.011, \\ \beta_{2;K_0^*} &= 1.091 \text{ GeV}, & P_{\chi^2_{\min}} &= 0.923671. \end{aligned} \quad (12)$$

The behavior of twist-2 DAs in different scenarios at $\mu_0 = 1$ GeV are also shown in Fig. 1. Meanwhile, QCDSRs [23] and CLF [49] based on Gegenbauer polynomials and truncations with $\mathcal{N} = 1$ (I) and $\mathcal{N} = 3$ (II) are also presented in Fig. 1. As can be seen from the Fig. 1, the two scenarios twist-2 DAs of our predictions exhibit similar behaviors to the two truncated forms from QCDSRs [23], respectively.

- For S1 case, the maximum value at $x = 0.096$ with $\phi_{2;K_0^*}^{(S1)}(x = 0.096) = 1.147$, the minimum value at $x = 0.908$ with $\phi_{2;K_0^*}^{(S1)}(x = 0.908) = -1.081$ and zero point at $x = 0.270, 0.512, 0.728$, respectively.
- For S2 case, the maximum value at $x = 0.140$ with $\phi_{2;K_0^*}^{(S2)}(x = 0.140) = 0.850$, the minimum value at $x = 0.860$ with $\phi_{2;K_0^*}^{(S2)}(x = 0.86) = -0.779$ and zero point at $x = 0.495$.
- These points indicate that there exist $SU_f(3)$ breaking effect, but the effect is relatively weak in $K_0^*(1430)$ -meson twist-2 DA.

As for the $K_0^*(1430)$ -meson twist-3 DAs $\phi_{3;K_0^*}^{p,\sigma}(x, \mu)$, we present the Gegenbauer moments at $\mu_k = 1.4$ GeV as

TABLE I: $D \rightarrow K_0^*(1430)$ TFFs at large recoil point $f_{\pm}(0)$ with two different $K_0^*(1430)$ -meson twist-2 DA scenarios. To make a comparison, we also listed other theoretical predictions.

	$f_+(0)$	$f_-(0)$
This work (S1)	$0.597^{+0.122}_{-0.121}$	$-0.136^{+0.023}_{-0.035}$
This work (S2)	$0.663^{+0.135}_{-0.134}$	$-0.202^{+0.026}_{-0.046}$
QCDSR [45]	0.57 ± 0.19	—
CLF [46]	0.48	—
GFM [47]	1.20 ± 0.07	—

follows [53]

$$\begin{aligned} a_{1,p}^{3;K_0^*}(\mu_k) &= 0.012 \pm 0.002, & a_{2,p}^{3;K_0^*}(\mu_k) &= 0.163 \pm 0.021, \\ a_{1,\sigma}^{\sigma;K_0^*}(\mu_k) &= 0.029 \pm 0.011, & a_{2,\sigma}^{3;K_0^*}(\mu_k) &= 0.019 \pm 0.004. \end{aligned} \quad (13)$$

When treating $D \rightarrow K_0^*(1430)$ TFFs, the continuum threshold s_0 is taken $4 \pm 0.1 \text{ GeV}^2$ [44], and the Borel window is taken $M^2 = 17 \pm 1 \text{ GeV}^2$ under the criterion of LCSR. Based on above parameters, we can get the $D \rightarrow K_0^*(1430)$ TFFs at large recoil point, which is presented in Table I and the results of QCDSR [45], CLF [46], and GFM [47] are used for comparison. In different twist-2 DAs, the contribution of the LCHO model $\phi_{2;K_0^*}^{(S2)}(x, \mu)$ is greater than truncated form $\phi_{2;K_0^*}^{(S1)}(x, \mu)$, which accounted for 21.0% and 12.2% of the $f_+(0)$ results, and 68.7% and 53.5% of $f_-(0)$ respectively. Our results is in a agreement with QCDSR [45].

Due to the mass of $K_0^*(1430)$, the physical allowable region in $D \rightarrow K_0^*(1430)\ell\nu_\ell$ is not large, *i.e.*, q^2 is from 0 to $(m_D - m_{K_0^*})^2 \approx 0.193 \text{ GeV}^2$, and the LCSR method is reliable in lower and intermediate region. So in the next step, we adopt the simplified series expansion (SSE) to extrapolate the f_{\pm} in whole kinematical region. The TFFs is expanded as

$$f_{\pm}(q^2) = \frac{1}{1 - q^2/m_D^2} \sum_{k=0,1,2} \beta_k z^k(q^2, t_0). \quad (14)$$

The β_k are real coefficients and the function $z^k(q^2, t_0) = (\sqrt{t_+ - q^2} - \sqrt{t_+ - t_0})/(\sqrt{t_+ - q^2} + \sqrt{t_+ - t_0})$ with $t_{\pm} = (m_D \pm m_{K_0^*})^2$ and $t_0 = t_+(1 - \sqrt{1 - t_-/t_+})$. Then, the behavior of TFF $f_{\pm}(q^2)$ in whole q^2 region can be determined which are shown in Fig. 2. In which, the solid line is our central value, the shadow band is our uncertainty, and the darker and lighter bands are the results of LCSR and SSE, respectively. At the same time, the behavior of $f_+(q^2)$ from QCDSR [45] and CLF [46] are also used for comparison. As shown in Fig. 2, compared with the prediction results of the two theoretical groups, the result of $f_+^{(S1)}(q^2)$ is in better agreement, and $f_+^{(S2)}(q^2)$ is larger than $f_+^{(S1)}(q^2)$ because of the greater contribution of twist-2 DA.

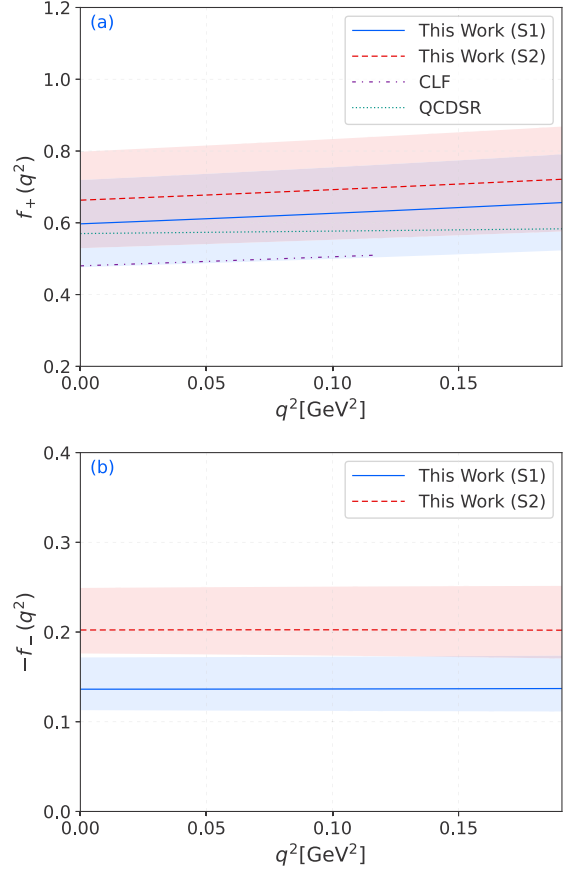


FIG. 2: The behavior of $D \rightarrow K_0^*(1430)$ TFFs $f_{\pm}(q^2)$ in whole kinematical region for S1 and S2 cases, and other predictions are given for comparison.

Subsequent step, we can obtain the differential decay width of $D \rightarrow K_0^*(1430)\ell\nu_\ell$ with $\ell = (e, \mu)$ through Eq. (4). In which, the CKM matrix element $|V_{cs}| = 0.975$ [61] and fermi coupling constant $G_F = 1.166 \times 10^{-5} \text{ GeV}^{-2}$. And special behavior is presented in Fig. 3, which shows that our results are in good agreement with QCDSR [45] whose mass of lepton e and μ is ignored. The total decay width can be calculated by integrating over q^2 in whole physical region $m_\ell^2 \leq q^2 \leq (m_D - m_{K_0^*})^2$. In different twist-2 DA cases, we have the following results,

$$\begin{aligned} \Gamma^{(S1)}(D \rightarrow K_0^*(1430)e\nu_e) &= (2.934^{+1.323}_{-1.068}) \times 10^{-16}, \\ \Gamma^{(S1)}(D \rightarrow K_0^*(1430)\mu\nu_\mu) &= (2.252^{+1.019}_{-0.823}) \times 10^{-16}, \\ \Gamma^{(S2)}(D \rightarrow K_0^*(1430)e\nu_e) &= (3.599^{+1.614}_{-1.306}) \times 10^{-16}, \\ \Gamma^{(S2)}(D \rightarrow K_0^*(1430)\mu\nu_\mu) &= (2.751^{+1.244}_{-1.008}) \times 10^{-16}. \end{aligned} \quad (15)$$

By using the the lifetime of the initial state $D^{0,+}$ -meson, $\tau_{D_0} = 0.41 \text{ ps}$ and $\tau_{D^+} = 1.03 \text{ ps}$, we can obtain the branching fractions for $D^{(0,+)} \rightarrow K_0^*(1430)^{(+,0)}\ell\nu_\ell$, which are presented in Table II. The results from QCDSR [45] and PDG [61] are also presented in it. In 2005, FOCUS collaboration [22] re-

FIG. 3: Differential decay widths of the $D \rightarrow K_0^*(1430)\ell\nu$ with $\ell = (e, \mu)$ for S1 and S2 cases. The result of QCDSR [45] is presented as a comparison.

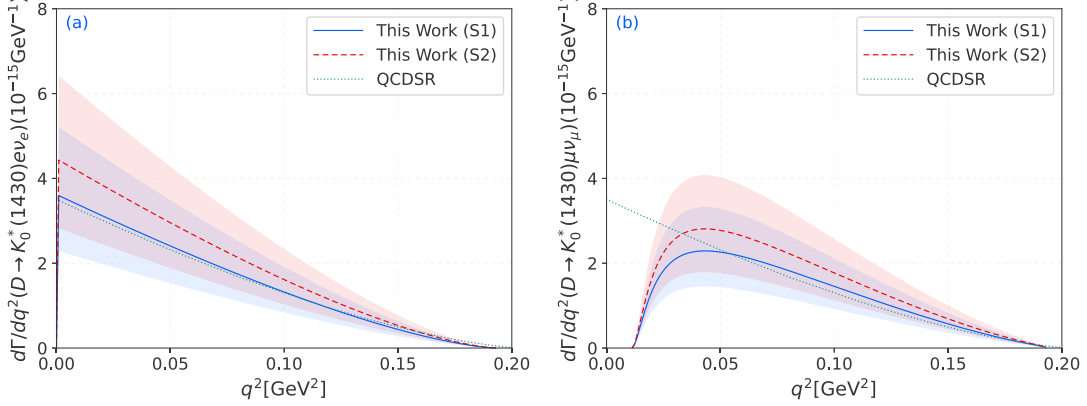


TABLE II: The predictions of the $D \rightarrow K_0^*(1430)\ell\nu$ branching fractions within uncertainties (in unit: 10^{-4}) for S1 and S2 cases. Meanwhile, the result of QCDSR [45], upper limits of PDG [61] and combining with FOCUS [62] and PDG [61] are used for comparison.

	$\mathcal{B}(D^0 \rightarrow K_0^*(1430)^+ e^- \bar{\nu}_e)$	$\mathcal{B}(D^+ \rightarrow K_0^*(1430)^0 e^+ \nu_e)$	$\mathcal{B}(D^0 \rightarrow K_0^*(1430)^+ \mu^- \bar{\nu}_\mu)$	$\mathcal{B}(D^+ \rightarrow K_0^*(1430)^0 \mu^+ \nu_\mu)$
This work (S1)	$1.83^{+0.82}_{-0.67}$	$4.59^{+2.07}_{-1.67}$	$1.40^{+0.64}_{-0.51}$	$3.52^{+1.60}_{-1.29}$
This work (S2)	$2.24^{+1.01}_{-0.81}$	$5.63^{+2.52}_{-2.04}$	$1.71^{+0.78}_{-0.63}$	$4.31^{+1.95}_{-1.58}$
PDG [61]	—	—	—	< 2.3
QCDSR [45]	$1.8^{+1.0}_{-1.5}$	$4.6^{+3.7}_{-2.6}$	$1.8^{+1.0}_{-1.5}$	$4.6^{+3.7}_{-2.6}$
FOCUS [62]+PDG [61]	—	—	—	$< 3.51^{+0.55}_{-0.54}$

ported the upper limit for $\Gamma(D^+ \rightarrow \bar{K}_0^*(1430)^0 \mu^+ \nu)$ by $\Gamma(D^+ \rightarrow \bar{K}_0^*(1430)^0 \mu^+ \nu)/\Gamma(D^+ \rightarrow K^- \pi^+ \mu^+ \nu) < 0.64\%$. Based on this, PDG [61] gives the upper limit of the branching fraction $\mathcal{B}(D^+ \rightarrow \bar{K}_0^*(1430)^0 \mu^+ \nu) < 2.3 \times 10^{-4}$. Our results are in good agreement with the theoretical values of QCDSR [45] within the error range. But, our results are larger than PDG [61]. At the same time, through literature research, we found that the upper limit of the branching ratio has another value. In 2004, the FOCUS Collaboration [62] reported the ratio $\Gamma(D^+ \rightarrow K \pi \mu^+ \nu_\mu)/\Gamma(D^+ \rightarrow \bar{K}^0 \mu^+ \nu_\mu) = 0.625 \pm 0.045 \pm 0.034$, and PDG [61] gives the average value of $\mathcal{B}(D^+ \rightarrow \bar{K}^0 \mu^+ \nu_\mu) = (8.76 \pm 0.07_{\text{stat}} \pm 0.18_{\text{sys}})\%$. So, we can get the $\mathcal{B}(D^+ \rightarrow K \pi \mu^+ \nu_\mu) = 5.48^{+0.87}_{-0.83}\%$ and further calculate $\mathcal{B}(D^+ \rightarrow \bar{K}_0^*(1430)^0 \mu^+ \nu) < 3.51^{+0.55}_{-0.54} \times 10^{-4}$ by the ratio 0.64%. Then, we can obviously see that the result of TF model $\phi_{2;K_0^*}^{(S1)}(x, \mu)$ is in a great agreement with it. At the same time, the branching fractions for the $D \rightarrow K_0^*(1430)\ell\nu_\ell$ decay channel is about 10 times than that of $D_s \rightarrow K_0^*(1430)\ell\nu_\ell$ of our previous work [48]. These results will make $D \rightarrow K_0^*(1430)\ell\nu_\ell$ decay channels more easily to be detected on BESIII collaboration.

Then, we decide to use the upper limit of the branching fractions $\mathcal{B}_{\text{max}}(D^+ \rightarrow K_0^*(1430)^0 \mu^+ \nu_\mu) = 3.49^{+0.55}_{-0.53} \times 10^{-4}$ to extract the CKM matrix element $|V_{cs}|$, which

are presented in Table III, and experimental predictions originate from PDG [61], BESIII [63–67], CLEO’09 [13] and HPQCD [68, 69] are also given in it. The above experimental results are within our error range. But, the central result under $\phi_{2;K_0^*}^{(S1)}(x, \mu)$ is in good agreement with BESIII’23 [64], and there is a certain gap with the average value of PDG [61]. This motivates us to anticipate more precise measurements of the branching ratio in future experiments.

Secondly, the lepton flavor universality $\mathcal{R}_{K_0^*}$ plays an important role in texting SM and exploring new physics, which have the following definition related to the decay width is

$$\mathcal{R}_{K_0^*}(q^2) = \frac{\int_{q_{\min}^2}^{q_{\max}^2} d\Gamma(D \rightarrow K_0^* \mu \nu_\mu)/dq^2}{\int_{q_{\min}^2}^{q_{\max}^2} d\Gamma(D \rightarrow K_0^* e \nu_e)/dq^2} \quad (16)$$

Then we presneted its trend changing with q^2 in Fig. 4. The results tend to infinity at the starting point and the end point respectively. Meanwhile, we predicted the results of $\mathcal{R}_{K_0^*}$,

$$\mathcal{R}_{K_0^*}^{(S1)} = 0.768^{+0.560}_{-0.368}, \quad \mathcal{R}_{K_0^*}^{(S2)} = 0.764^{+0.555}_{-0.365}. \quad (17)$$

The slight discrepancies in the numerical results under the two models may be attributed to the the fact that

TABLE III: The prediction of $|V_{cs}|$ from $D^+ \rightarrow K_0^{*(1430)0} \mu^+ \nu_\mu$ within uncertainties for S1 and S2 cases. Other experimental results are listed here for comparison.

	$ V_{cs} $
This work (S1)	$0.997^{+0.265}_{-0.187}$
This work (S2)	$0.903^{+0.239}_{-0.169}$
PDG [61]	0.975 ± 0.006
BESIII'15 [67]	$0.975 \pm 0.008 \pm 0.015 \pm 0.025$
BESIII'17 [63]	$0.944 \pm 0.005 \pm 0.015 \pm 0.024$
BESIII'23 [64]	$0.993 \pm 0.015 \pm 0.012 \pm 0.004$
BESIII'24 [65]	$1.011 \pm 0.014 \pm 0.018 \pm 0.003$
BESIII'24 [66]	$0.968 \pm 0.010 \pm 0.009$
CLEO'09 [13]	$0.985 \pm 0.009 \pm 0.006 \pm 0.103$
HPQCD'13 [68]	$1.017(63)$
HPQCD'21 [69]	$0.9663(53)(39)(19)(40)$

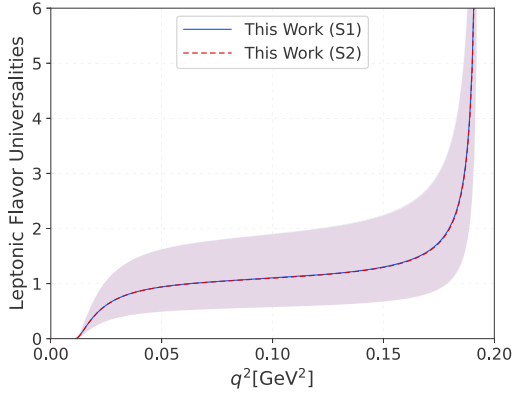


FIG. 4: The lepton flavor universality $R_{K_0^*}$ for $D \rightarrow K_0^{*(1430)} \ell \nu_\ell$ as function of q^2 for S1 and S2 cases.

the extrapolation trend of the TFFs $f_\pm(q^2)$ cannot be completely consistent.

Finally, we calculate three angular observables. The different forward-backward asymmetries, lepton polarization asymmetries and flat terms of $D \rightarrow K_0^* \ell \nu_\ell$ with $\ell = (e, \mu)$ are displayed in Fig. 5. One can see that the behaviors of three observables are highly consistent under the two twist-2 DA models and only subtle differences can be seen in the curve of $\mu \nu_\mu$ channel. This may be because these observables are the ratio function of TFFs. The trend of TFFs with q^2 under the two DAs has a good consistency. There exists a ratio in terms of numerical values, where the contribution of $f_-(q^2)$ is very small. We can assume that the contribution of $f_-(q^2)$ is negligible. It can be seen from Eq. (5) that the ratio will be reduced. Therefore, the results of these angular observables under the two DAs have certain consistency, and the contribution of $f_-(q^2)$ also leads to subtle differ-

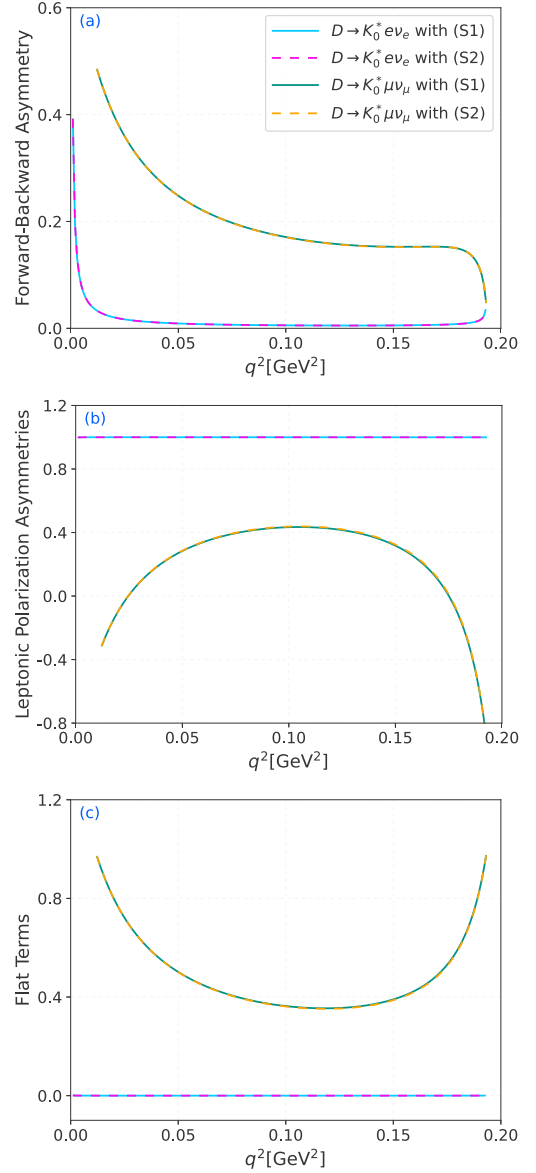


FIG. 5: The different forward-backward asymmetries, lepton polarization asymmetries and flat terms of $D \rightarrow K_0^* \ell \nu_\ell$ for S1 and S2 cases.

ences in the final results. Moreover, due to the mass size of electron and muon, the results from the $e \nu_e$ channel can be regarded as identical. In addition, there are significant differences in these differential observables when $\ell = e$ and $\ell = \mu$ respectively, suggesting that these observables are highly sensitive to the mass of the lepton. Then, the integrated results of the three angular observables are listed in Table IV. It is evident that \mathcal{A}_{FB} and \mathcal{F}_H are proportional to the square of the lepton mass, while $\mathcal{A}_{\lambda_\ell}$ is inversely proportional to the lepton mass. Additionally, the integral results of all these quantities are close to 0.

TABLE IV: The integrated results of the three angular observables for the S1 and S2 cases.

	This work (S1)	This work (S2)
$\mathcal{A}_{\text{FB}}(10^{-6})$	$5.39^{+3.93}_{-2.58}$	$5.38^{+3.91}_{-2.57}$
$\mathcal{A}_{\text{FB}}(10^{-2})$	$3.75^{+2.75}_{-1.80}$	$3.75^{+2.75}_{-1.80}$
$\mathcal{A}_{\lambda\ell}(10^{-1})$	$1.94^{+0.00}_{-0.00}$	$1.94^{+0.00}_{-0.00}$
$\mathcal{A}_{\lambda\ell}(10^{-2})$	$3.95^{+6.91}_{-10.6}$	$4.03^{+6.87}_{-10.5}$
$\mathcal{F}_{\text{H}}(10^{-5})$	$1.47^{+1.08}_{-0.71}$	$1.46^{+1.06}_{-0.71}$
$\mathcal{F}_{\text{H}}(10^{-2})$	$8.95^{+6.59}_{-4.32}$	$8.92^{+6.55}_{-4.30}$

IV. SUMMARY

In this paper, we investigated the semileptonic decay $D \rightarrow K_0^*(1430)\ell\nu_\ell$ with $\ell = (e, \mu)$. Firstly, the TFFs for $D \rightarrow K_0^*(1430)$ are calculated by using LCSR approach. Considering that the distribution amplitude is the main non-perturbative input in LCSR, we adopt two different twist-2 DAs for calculation and comparison, *i.e.*, $\phi_{2;K_0^*}^{(S1)}(x, \mu)$ and $\phi_{2;K_0^*}^{(S2)}(x, \mu)$ based on truncated form and LCHO model, respectively. The relevant numerical results of $f_\pm(0)$ are listed in Table I. Compared with $\phi_{2;K_0^*}^{(S2)}(x, \mu)$, the $f_+(0)$ by using $\phi_{2;K_0^*}^{(S1)}(x, \mu)$ is more consistent with QCDSR [45]. Then the TFFs are extrapolated to high q^2 -region by using $z(q^2, t)$ converging the SSE, whose behavior is shown in Fig 2, which includes the results of other groups. After extrapolating the TFFs, the differential decay width of $D^{(0,+)} \rightarrow K_0^*(1430)^{(+,0)}\ell\nu_\ell$ with $\ell = (e, \mu)$ are obtained and presented it in Fig. 3. The corresponding branching fractions are also listed in Table II. Our predictions are in good agreement with QCDSR [45], but for the value of $\mathcal{B}(D^+ \rightarrow K_0^*(1430)^0\mu^+\nu_\mu)$ is still different from PDG [61]. Meanwhile, we give a new upper limit of $\mathcal{B}(D^+ \rightarrow K_0^*(1430)^0\mu^+\nu)$ by using the proportional relationship of $\Gamma(D^+ \rightarrow K\pi\mu^+\nu_\mu)/\Gamma(D^+ \rightarrow \bar{K}^0\mu^+\nu_\mu)$, $\Gamma(D^+ \rightarrow \bar{K}_0^*(1430)^0\mu^+\nu)/\Gamma(D^+ \rightarrow K^-\pi^+\mu^+\nu)$, and the

world average result of $\mathcal{B}(D^+ \rightarrow \bar{K}^0\mu^+\nu_\mu)$, which is in good agreement with our result in first twist-2 DA scenario. Then, this branching fraction is used to calculate the CKM matrix $|V_{cs}|$. The prediction under $\phi_{2;K_0^*}^{(S1)}(x, \mu)$ is in great agreement with BESIII'23 [64]. Furthermore, we predicted the ratio $\mathcal{R}_{K_0^*}^{(S1)} = 0.768^{+0.560}_{-0.368}$, $\mathcal{R}_{K_0^*}^{(S2)} = 0.764^{+0.555}_{-0.365}$.

Finally, the three angular observables, forward-backward asymmetries \mathcal{A}_{FB} , lepton polarization asymmetries $\mathcal{A}_{\lambda_\ell}$ and q^2 -differential flat terms \mathcal{F}_{H} are also calculated, whose differential results of these observables as a function of q^2 are shown in Fig. 5. Simultaneously, the numerical results after integration are listed in Table IV. The semileptonic decays of $D \rightarrow K_0^*(1430)\ell\nu_\ell$ with $\ell = (e, \mu)$ are meaningful decay channel. These interesting observables can help us better understand the structure of scalar mesons, and provide valuable information for testing the SM and finding BSM. According to the current experimental data, in this decay process, the predicted observable under $\phi_{2;K_0^*}^{(S1)}(x, \mu)$ are more accurate. Because of different decay processes, the application of different amplitude models will have different effects, so this is within our expected results. But we still eagerly anticipate that this decay channel will be detected by experimental collaborations and give more accurate results in the near future.

V. ACKNOWLEDGMENTS

This work was supported in part by the National Natural Science Foundation of China under Grant No. 12265009, No. 12265010, No. 12265011 and No.12347101, the Project of Guizhou Provincial Department of Science and Technology under Grant No. ZK[2023]024, No. YQK[2023]016 and No. ZK[2023]141.

-
- [1] J. Y. Ge *et al.* [CLEO Collaboration], Study of $D^0 \rightarrow \pi^-e^+\nu_e$, $D^+ \rightarrow \pi^0e^+\nu_e$, $D^0 \rightarrow K^-e^+\nu_e$, and $D^+ \rightarrow \bar{K}^0e^+\nu_e$ in Tagged Decays of the $\psi(3770)$ Resonance, *Phys. Rev. D* **79** (2009), 052010. [arXiv:0810.3878]
 - [2] K. Liu [BESIII Collaboration], Semileptonic and leptonic D decays at BESIII, *PoS LeptonPhoton2019* (2019), 046.
 - [3] S. Zhang [BESIII Collaboration], Test lepton flavor universality with (semi)leptonic D decays at BESIII, *SciPost Phys. Proc.* **1** (2019), 016.
 - [4] Y. H. Yang [BESIII Collaboration], (Semi-)leptonic decays of D Mesons at BESIII. [arXiv:1812.00320]
 - [5] M. Ablikim *et al.* [BESIII Collaboration], Improved measurement of the absolute branching fraction of

- $D^+ \rightarrow \bar{K}^0\mu^+\nu_\mu$, *Eur. Phys. J. C* **76** (2016) no.7, 369. [arXiv:1605.00068]
- [6] M. Ablikim *et al.* [BESIII Collaboration], Determination of the absolute branching fractions of $D^0 \rightarrow K^-e^+\nu_e$ and $D^+ \rightarrow \bar{K}^0e^+\nu_e$, *Phys. Rev. D* **104** (2021) no.5, 052008. [arXiv:2104.08081]
- [7] M. Ablikim *et al.* [BESIII Collaboration], Study of Dynamics of $D^0 \rightarrow K^-e^+\nu_e$ and $D^0 \rightarrow \pi^-e^+\nu_e$ Decays, *Phys. Rev. D* **92** (2015) no.7, 072012. [arXiv:1508.07560]
- [8] M. Ablikim *et al.* [BESIII Collaboration], Observation of the decay $D^0 \rightarrow \rho^-\mu^+\nu_\mu$, *Phys. Rev. D* **104** (2021) no.9, L091103. [arXiv:2106.02292]

- [9] M. Ablikim *et al.* [BESIII Collaboration], Measurement of the form factors in the decay $D^+ \rightarrow \omega e^+ \nu_e$ and search for the decay $D^+ \rightarrow \phi e^+ \nu_e$, *Phys. Rev. D* **92** (2015) no.7, 071101. [arXiv:1508.00151]
- [10] S. Dobbs *et al.* [CLEO Collaboration], First Measurement of the Form Factors in the Decays $D^0 \rightarrow \rho^- e^+ \nu_e$ and $D^+ \rightarrow \rho^0 e^+ \nu_e$, *Phys. Rev. Lett.* **110** (2013) no.13, 131802. [arXiv:1112.2884]
- [11] G. S. Huang *et al.* [CLEO Collaboration], Study of semileptonic charm decays $D^0 \rightarrow \pi^- \ell^+ \nu$ and $D^0 \rightarrow K^- \ell^+ \nu$, *Phys. Rev. Lett.* **94** (2005), 011802. [arXiv:0407035]
- [12] J. Yelton *et al.* [CLEO Collaboration], Absolute Branching Fraction Measurements for Exclusive D_s Semileptonic Decays, *Phys. Rev. D* **80** (2009), 052007. [arXiv:0903.0601]
- [13] D. Besson *et al.* [CLEO Collaboration], Improved measurements of D meson semileptonic decays to π and K mesons, *Phys. Rev. D* **80** (2009), 032005. [arXiv:0906.2983]
- [14] G. S. Huang *et al.* [CLEO Collaboration], Absolute branching fraction measurements of exclusive D^+ semileptonic decays, *Phys. Rev. Lett.* **95** (2005), 181801. [arXiv:0506053]
- [15] M. Ablikim *et al.* [BESIII Collaboration], Observation of $D^+ \rightarrow f_0(500) e^+ \nu_e$ and Improved Measurements of $D \rightarrow \rho e^+ \nu_e$, *Phys. Rev. Lett.* **122** (2019) no.6, 062001. [arXiv:1809.06496]
- [16] M. Ablikim *et al.* [BESIII Collaboration], Observation of the Semileptonic Decay $D^0 \rightarrow a_0(980)^- e^+ \nu_e$ and Evidence for $D^+ \rightarrow a_0(980)^0 e^+ \nu_e$, *Phys. Rev. Lett.* **121** (2018) no.8, 081802. [arXiv:1803.02166]
- [17] M. Ablikim *et al.* [BESIII Collaboration], Study of the $f_0(980)$ and $f_0(500)$ Scalar Mesons through the Decay $D_s^+ \rightarrow \pi^+ \pi^- e^+ \nu_e$, *Phys. Rev. Lett.* **132** (2024) no.14, 141901. [arXiv:2303.12927]
- [18] M. Ablikim *et al.* [BESIII Collaboration], Study of light scalar mesons through $D_s^+ \rightarrow \pi^0 \pi^0 e^+ \nu_e$ and $K_S^0 K_S^{*0} e^+ \nu_e$ decays, *Phys. Rev. D* **105**, no.3, L031101 (2022). [arXiv:2110.13994]
- [19] M. Ablikim *et al.* [BESIII Collaboration], Studies of the decay $D_s^+ \rightarrow K^+ K^- \mu^+ \nu_\mu$, *JHEP* **12**, 072 (2023). [arXiv:2307.03024]
- [20] M. Ablikim *et al.* [BESIII Collaboration], Search for the decay $D_s^+ \rightarrow a_0(980)^0 e^+ \nu_e$, *Phys. Rev. D* **103**, no.9, 092004 (2021). [arXiv:2103.11855]
- [21] K. M. Ecklund *et al.* [CLEO Collaboration], Study of the semileptonic decay $D_s^+ \rightarrow f_0(980) e^+ \nu$ and implications for $B_s^0 \rightarrow J/\psi f_0$, *Phys. Rev. D* **80**, 052009 (2009). [arXiv:0907.3201]
- [22] J. M. Link *et al.* [FOCUS Collaboration], Hadronic mass spectrum analysis of $D^+ \rightarrow K^- \pi^+ \mu^+ \nu$ decay and measurement of the $K^*(892)^0$ mass and width, *Phys. Lett. B* **621** (2005), 72-80. [arXiv:0503043]
- [23] H. Y. Cheng, C. K. Chua and K. C. Yang, Charmless hadronic B decays involving scalar mesons: Implications to the nature of light scalar mesons, *Phys. Rev. D* **73** (2006), 014017. [arXiv:0508104]
- [24] R. L. Jaffe, Multi-Quark Hadrons. 1. The Phenomenology of (2 Quark 2 anti-Quark) Mesons, *Phys. Rev. D* **15** (1977), 267.
- [25] J. D. Weinstein and N. Isgur, $K\bar{K}$ Molecules, *Phys. Rev. D* **41** (1990), 2236.
- [26] J. D. Weinstein and N. Isgur, Do Multi-Quark Hadrons Exist? *Phys. Rev. Lett.* **48** (1982), 659.
- [27] J. D. Weinstein and N. Isgur, The $qq\bar{q}\bar{q}$ System in a Potential Model, *Phys. Rev. D* **27** (1983), 588.
- [28] N. A. Tornqvist, Scalar Mesons in the Unitarized Quark Model, *Phys. Rev. Lett.* **49** (1982), 624-627.
- [29] R. L. Jaffe, Multi-Quark Hadrons. 2. Methods, *Phys. Rev. D* **15** (1977), 281.
- [30] A. L. Kataev, QCD sum rules and radial excitations of light pseudoscalar and scalar mesons, *Phys. Atom. Nucl.* **68** (2005), 567-572. [arXiv:0406305]
- [31] J. Vijande, A. Valcarce, F. Fernandez and B. Silvestre-Brac, Nature of the light scalar mesons, *Phys. Rev. D* **72** (2005), 034025. [arXiv:0508142]
- [32] H. J. Lee, Discussion on Scalar Meson $a_0(980)$ as a Tetraquark State with the QCD Sum Rules including the Contribution from Instanton, *New Phys. Sae Mulli* **72** (2022) no.12, 887-892.
- [33] T. Humanic [ALICE Collaboration], Studying the $a_0(980)$ tetraquark candidate using $K_s^0 K^\pm$ interactions in the LHC ALICE collaboration, *Rev. Mex. Fis. Suppl.* **3** (2022) no.3, 0308039.
- [34] T. V. Brito, F. S. Navarra, M. Nielsen and M. E. Bracco, QCD sum rule approach for the light scalar mesons as four-quark states, *Phys. Lett. B* **608** (2005), 69-76. [arXiv:0411233]
- [35] C. Alexandrou, J. Berlin, M. Dalla Brida, J. Finkenrath, T. Leontiou and M. Wagner, Lattice QCD investigation of the structure of the $a_0(980)$ meson, *Phys. Rev. D* **97** (2018) no.3, 034506. [arXiv:1711.09815]
- [36] E. Klempt and A. Zaitsev, Glueballs, Hybrids, Multiquarks. Experimental facts versus QCD inspired concepts, *Phys. Rept.* **454** (2007), 1-202. [arXiv:0708.4016]
- [37] T. M. Aliev, K. Azizi and M. Savci, Analysis of rare $B \rightarrow K_0^*(1430) \ell^+ \ell^-$ decay within QCD sum rules, *Phys. Rev. D* **76** (2007), 074017. [arXiv:0710.1508]
- [38] M. J. Aslam, C. D. Lu and Y. M. Wang, $B \rightarrow K_0^*(1430) \ell^+ \ell^-$ decays in supersymmetric theories, *Phys. Rev. D* **79** (2009), 074007. [arXiv:0902.0432]
- [39] Y. J. Sun, Z. H. Li and T. Huang, $B_{(s)} \rightarrow S$ transitions in the light cone sum rules with the chiral current, *Phys. Rev. D* **83** (2011), 025024. [arXiv:1011.3901]
- [40] Z. G. Wang, $B - S$ transition form-factors with the light-cone QCD sum rules, *Eur. Phys. J. C* **75** (2015) no.2, 50. [arXiv:1409.6449]
- [41] Z. G. Wang, Semi-leptonic $B \rightarrow S$ decays in the standard model and in the universal extra dimension model, *Nucl. Phys. B* **898** (2015), 431-447. [arXiv:1411.7961]
- [42] R. Khosravi, Semileptonic $B_s \rightarrow K_0^*(1430)$ transitions with the light-cone sum rules, *Phys. Rev. D* **105** (2022) no.11, 116027. [arXiv:2203.09997]
- [43] R. Khosravi, Form factors of $B_{(s)}$ to light scalar mesons with the B-meson light-cone sum rules, *Phys. Rev. D* **109** (2024) no.3, 036003. [arXiv:2401.05155]
- [44] D. S. Du, J. W. Li and M. Z. Yang, Mass and decay constant of $I = 1/2$ scalar meson in QCD sum rule, *Phys. Lett. B* **619** (2005), 105-114. [arXiv:0409302]

- [45] M. Z. Yang, Semileptonic decay of B and $D \rightarrow K_0^*(1430)\ell\nu$ from QCD sum rule, *Phys. Rev. D* **73** (2006), 034027. [arXiv:0509103]
- [46] H. Y. Cheng, C. K. Chua and C. W. Hwang, Covariant light front approach for s wave and p wave mesons: Its application to decay constants and form-factors, *Phys. Rev. D* **69** (2004), 074025. [arXiv:0310359]
- [47] H. Y. Cheng, Hadronic D decays involving scalar mesons, *Phys. Rev. D* **67** (2003), 034024. [arXiv:0212117]
- [48] D. Huang, T. Zhong, H. B. Fu, Z. H. Wu, X. G. Wu and H. Tong, $K_0^*(1430)$ twist-2 distribution amplitude and $B_s, D_s \rightarrow K_0^*(1430)$ transition form factors, *Eur. Phys. J. C* **83** (2023) no.7, 680. [arXiv:2211.06211]
- [49] L. Chen, M. Zhao, Y. Zhang and Q. Chang, Study of $B_{u,d,s} \rightarrow K_0^*(1430)P$ and $K_0^*(1430)V$ decays within QCD factorization, *Phys. Rev. D* **105** (2022) no.1, 016002. [arXiv:2112.00915]
- [50] J. Hua *et al.* [Lattice Parton], Pion and Kaon Distribution Amplitudes from Lattice QCD, *Phys. Rev. Lett.* **129** (2022) no.13, 132001. [arXiv:2201.09173]
- [51] P. Ball, V. M. Braun and A. Lenz, Twist-4 distribution amplitudes of the K^* and ϕ mesons in QCD, *JHEP* **08** (2007), 090. [arXiv:0707.1201]
- [52] J. Hua *et al.* [Lattice Parton], Distribution Amplitudes of K^* and ϕ at the Physical Pion Mass from Lattice QCD, *Phys. Rev. Lett.* **127** (2021) no.6, 062002. [arXiv:2011.09788]
- [53] H. Y. Han, X. G. Wu, H. B. Fu, Q. L. Zhang and T. Zhong, Twist-3 Distribution Amplitudes of Scalar Mesons within the QCD Sum Rules and Its Application to the $B \rightarrow S$ Transition Form Factors, *Eur. Phys. J. A* **49** (2013), 78. [arXiv:1301.3978]
- [54] D. Becirevic, S. Fajfer, I. Nisandzic and A. Tayduganov, Angular distributions of $\bar{B} \rightarrow D^{(*)}\ell\bar{\nu}_\ell$ decays and search of New Physics, *Nucl. Phys. B* **946** (2019), 114707. [arXiv:1602.03030]
- [55] B. Y. Cui, Y. K. Huang, Y. L. Shen, C. Wang and Y. M. Wang, Precision calculations of $B_{d,s} \rightarrow \pi, K$ decay form factors in soft-collinear effective theory, *JHEP* **03** (2023), 140. [arXiv:2212.11624]
- [56] Y. M. Wang, M. J. Aslam and C. D. Lu, Scalar mesons in weak semileptonic decays of $B_{(s)}$, *Phys. Rev. D* **78** (2008), 014006. [arXiv:0804.2204]
- [57] T. Zhong, H. B. Fu and X. G. Wu, Investigating the ratio of CKM matrix elements $|V_{ub}|/|V_{cb}|$ from semileptonic decay $B_s^0 \rightarrow K^-\mu^+\nu_\mu$ and kaon twist-2 distribution amplitude, *Phys. Rev. D* **105** (2022) no.11, 116020. [arXiv:2201.10820]
- [58] T. Zhong, Z. H. Zhu, H. B. Fu, X. G. Wu and T. Huang, Improved light-cone harmonic oscillator model for the pionic leading-twist distribution amplitude, *Phys. Rev. D* **104** (2021) no.1, 016021. [arXiv:2102.03989]
- [59] C. D. Lu, Y. M. Wang and H. Zou, Twist-3 distribution amplitudes of scalar mesons from QCD sum rules, *Phys. Rev. D* **75** (2007), 056001. [arXiv:0612210]
- [60] S. Kuberski, F. Joswig, S. Collins, J. Heitger and W. Söldner, D and D_s decay constants in $N_f = 2 + 1$ QCD with Wilson fermions. [arXiv:2405.04506]
- [61] S. Navas *et al.* [Particle Data Group], *Phys. Rev. D* **110** (2024) no.3, 030001.
- [62] J. M. Link *et al.* [FOCUS Collaboration], Measurement of the ratio of the vector to pseudoscalar charm semileptonic decay rate $\Gamma(D^+ \rightarrow \bar{K}^{*0}\mu^+\nu_\mu)/\Gamma(D^+ \rightarrow \bar{K}^0\mu^+\nu_\mu)$, *Phys. Lett. B* **598** (2004), 33-41. [arXiv:0406060]
- [63] M. Ablikim *et al.* [BESIII Collaboration], Analysis of $D^+ \rightarrow \bar{K}^0 e^+\nu_e$ and $D^+ \rightarrow \pi^0 e^+\nu_e$ semileptonic decays, *Phys. Rev. D* **96** (2017) no.1, 012002. [arXiv:1703.09084]
- [64] M. Ablikim *et al.* [BESIII Collaboration], Updated measurement of the branching fraction of $D_s^+ \rightarrow \tau^+\nu_\tau$ via $\tau^+ \rightarrow \pi^+\bar{\nu}_\tau$, *Phys. Rev. D* **108** (2023) no.9, 092014. [arXiv:2303.12600]
- [65] M. Ablikim *et al.* [BESIII Collaboration], Measurement of the branching fraction of $D_s^+ \rightarrow \ell^+\nu_\ell$ via $e^+e^- \rightarrow D_s^{*+}D_s^{*-}$, [arXiv:2407.11727]
- [66] P. L. Liu [BESIII Collaboration], $|V_{cs}|$ determination and LFU test in charm decays at BESIII. [arXiv:2405.08376]
- [67] M. Ablikim *et al.* [BESIII Collaboration], Study of decay dynamics and CP asymmetry in $D^+ \rightarrow K_L^0 e^+\nu_e$ decay, *Phys. Rev. D* **92** (2015) no.11, 112008. [arXiv:1510.00308]
- [68] G. C. Donald *et al.* [HPQCD Collaboration], V_{cs} from $D_s \rightarrow \phi\ell\nu$ semileptonic decay and full lattice QCD, *Phys. Rev. D* **90** (2014) no.7, 074506. [arXiv:1311.6669]
- [69] B. Chakraborty *et al.* [(HPQCD Collaboration) and HPQCD], Improved V_{cs} determination using precise lattice QCD form factors for $D \rightarrow K\ell\nu$, *Phys. Rev. D* **104** (2021) no.3, 034505. [arXiv:2104.09883]